PHYSICAL REVIEW B, VOLUME 63, 041103(R)

Observation of dynamic coupling between the Q_1 and Q_2 charge-density waves in $NbSe_3$

Y. Li, D. Y. Noh,* J. H. Price, K. L. Ringland, and J. D. Brock
School of Applied and Engineering Physics, Cornell University, Ithaca, New York 14853

S. G. Lemay, K. Cicak, and R. E. Thorne
Laboratory of Atomic and Solid State Physics, Cornell University, Ithaca, New York 14853

Mark Sutton
Center for the Physics of Materials and Department of Physics, McGill University, Montreal H3A 2T8, Canada

(Received 6 October 2000; published 9 January 2001)

We report synchrotron based high-resolution x-ray scattering and *in situ* electronic transport measurements of the Q_1 and Q_2 charge-density waves (CDW's) in $NbSe_3$ as a function of applied electric field in the low-temperature ''switching'' regime. Detailed analysis of the line shape of the x-ray satellite peaks demonstrates that the Q_2 CDW changes state when it depins at E_T but does not exhibit any abrupt structural change at E_T^*, where the collective CDW current abruptly increases. In contrast, the Q_1 CDW does not exhibit structural changes at E_T but abruptly changes state at E_T^* to a structure very similar to the structure of the sliding Q_1 at high temperatures. These data demonstrate coupling between the Q_2 and Q_1 CDW's.

DOI: 10.1103/PhysRevB.63.041103 PACS number(s): 71.45.Lr, 61.10.−i

A charge-density wave (CDW) in the presence of an applied electric field is the prototypic example of a driven periodic system with many internal degrees of freedom interacting with quenched random disorder. In the simplest case, the CDW state consists of a sinusoidal variation of the conduction-electron density and a concomitant sinusoidal lattice-distortion wave (LDW),[1] $\boldsymbol{u}(\boldsymbol{r},t)=\boldsymbol{u}_0\sin[\boldsymbol{Q}\cdot\boldsymbol{r}+\phi(\boldsymbol{r},t)]$. Here, $Q=2k_F$, k_F is the Fermi wave number and $\phi(\boldsymbol{r},t)$ allows the CDW to make small local distortions in order to adapt energetically to impurities or other crystal defects. In the absence of an applied electric field, quenched random disorder destroys the long-range order of the CDW state.[2] Applying an electric field greater than a threshold value E_T causes the CDW to ''depin'' and begin sliding coherently. This collective mode is responsible for the nonlinear electronic transport commonly associated with CDW's.[3]

$NbSe_3$ has two CDW transitions: $T_{p1}=144$ K and $T_{p2}=59$ K. The low-temperature phase diagram for $NbSe_3$ is schematically illustrated in Fig. 1. Below about $\frac{2}{3}T_{p2}$, for applied electric fields, $E<E_T$ (region I), both CDW's remain pinned. In the range $E_T<E<E_T^*$ (region II), a very small CDW current j_c with a strikingly slow but coherent collective CDW motion is observed.[4] At a nearly temperature-independent field E_T^*, j_c jumps by several orders of magnitude. This jump is called switching and is accompanied by other effects such as hysteresis, delayed conduction, and period-doubling to chaos[5–7]. Switching is observed in many CDW systems such as $K_{0.3}MoO_3$,[8,9] TaS_3,[8,10] and $NbSe_3$,[11,12] and is believed to be a fundamental property of CDW dynamics. Although many models have been proposed,[11,13–16] the mechanism for switching, especially in $NbSe_3$ which remains semimetallic, is still not fully understood.

The wave vectors of the coexisting CDW's are $\boldsymbol{Q}_1=(0\ \ 0.243\ \ 0)$ and $\boldsymbol{Q}_2=(0.5\ \ 0.26\ \ 0.5)$.[17,18] The approximate relation

$$2(\boldsymbol{Q}_1+\boldsymbol{Q}_2)\approx(111) \tag{1}$$

strongly suggests that any infinitesimal coupling would drive a ''lock-in'' transition.[19–21] However, both electronic transport[22] and x-ray scattering measurements[23] on *pinned* CDW's showed no sign of a lock-in transition. Here, we report high-resolution synchrotron x-ray diffraction measurements of the transverse structure of both CDW's and *in situ* electronic transport measurements at electric fields ranging from zero to greater than E_T^*. We find that the Q_2 CDW begins to disorder continuously at E_T, evolving into a structure identical to that of the sliding Q_1 CDW at temperatures above T_{p2}.[24] The Q_2 CDW does not exhibit an abrupt structural change at E_T^*. In contrast, the Q_1 CDW abruptly disorders at E_T^*, changing to the sliding state structure observed at higher temperatures. These data imply that Q_1 and Q_2 are dynamically coupled.

X rays are nearly ideal for studying the structure of CDW's because they couple directly to the LDW. For the simple sinusoidal LDW considered above, the static structure factor of the CDW satellite is given by

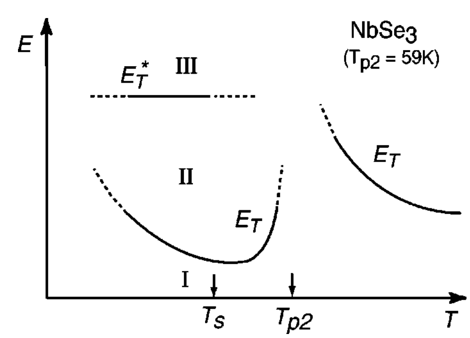

FIG. 1. Schematic phase diagram. In region I, both CDW's stay pinned; in region II (slow branch) Q_2 CDW starts to slide; in region III CDW conduction switches to fast branch. Below T_s ($\sim\frac{2}{3}T_{p2}$), the system enters the low temperature switching regime.

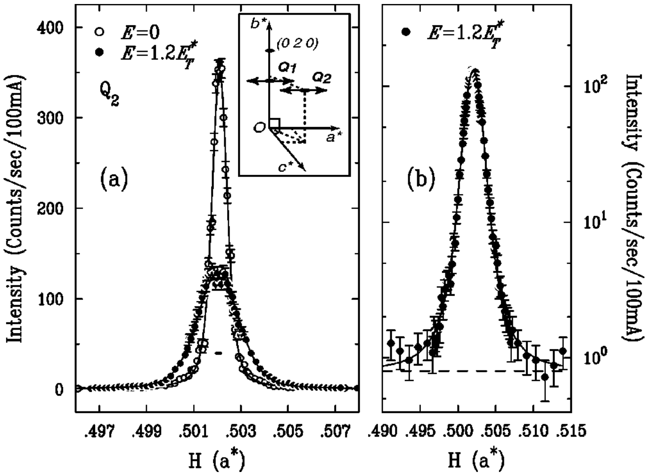

FIG. 2. (a) Transverse scans of the Q_2 CDW along the ***a*** direction at zero field (open circles) and at $E=1.2E_T^*$ (filled circles) at 35K. The horizontal bar under the peak indicates the instrumental resolution. Inset: schematic of reciprocal space and scan directions. (b) Semilog plot of the sliding state data with the best fit (solid lines) to the line shape given in the text. The best fit values of the parameters are $\alpha=0.80\pm0.01$ and $\xi=1.47\pm0.01\times10^3$ Å, $\chi^2=1.1$. The dashed line indicates the measured background.

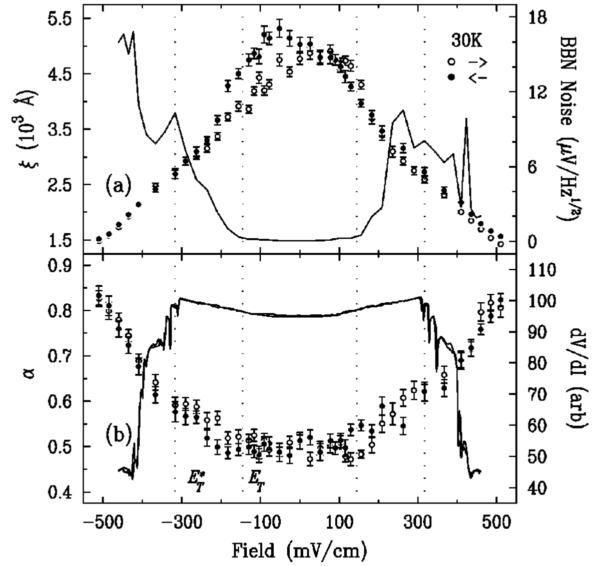

FIG. 3. (a) Correlation length ξ of the Q_2 CDW and BBN measured at 30 K. (b) Phase roughness exponent α of the Q_2 CDW and dV/dI. The two dashed lines indicate E_T and E_T^*, respectively. Open (filled) circles correspond to sweeping the applied field in the positive (negative) direction.

$$\mathcal{S}(\boldsymbol{q},t)\sim\int d^3\boldsymbol{r}\int d^3\boldsymbol{r}'\,e^{i(\boldsymbol{q}-\boldsymbol{G}\pm\boldsymbol{Q})\cdot(\boldsymbol{r}-\boldsymbol{r}')}e^{-g(\boldsymbol{r}-\boldsymbol{r}',t)}, \quad (2)$$

where $e^{-g(\boldsymbol{r}-\boldsymbol{r}',t)}=\langle e^{i\phi(\boldsymbol{r},t)}e^{-i\phi(\boldsymbol{r}',t)}\rangle$ is the phase-phase correlation function averaged over the impurity distribution, $\boldsymbol{q}$ is the x-ray scattering vector, and $\boldsymbol{G}$ is a reciprocal-lattice vector.

X-ray measurements were performed both on beam line X20A at the National Synchrotron Light Source (NSLS) and on beam line 8-ID at the Advanced Photon Source (APS). On X20A, 8.25 keV x rays were selected by a double-bounce Ge(111) Bragg monochromator from the white beam generated by a bending magnet. The illuminated spot size was set by 0.4 mm wide slits in one direction and by the sample width ($\sim$10 μm) in the other direction. The angular divergence of the source (0.012°) and the crystal mosaic (0.010° for the chosen crystals) set the effective transverse (θ) resolution. On 8-ID, 7.66 keV x rays were selected by a diamond (111) Bragg monochromator from the beam generated by an undulator. Due to the much smaller source size (50 μm) and longer source-station distance (55 m), the angular divergence in the (vertical) scattering plane is 20 times smaller than at the NSLS. A pair of highly polished slits set the spot size to be 27.5 μm along the whisker axis. This produces a coherent and intense x-ray beam at the sample.[25] The samples were mounted across a 3 mm diameter hole in an alumina substrate with four-probe patterned contacts, and surrounded by helium exchange gas. The high-quality pure $NbSe_3$ whiskers used had residual resistance ratios $\sim$300 and excellent mode-locking[26] of the Q_1 CDW above T_{p2}. Scans were taken in transmission mode with the scattering vector constrained to lie in the plane defined by $\boldsymbol{a}^*$ and $\boldsymbol{b}^*$ as illustrated in the inset to Fig. 2(a).

Figure 2(a) shows typical x-ray scattering scans collected on X20A in the $\boldsymbol{a}^*$ direction through the Q_2 (0.5 1.263 0.5) satellite, at both zero field (ZF) and $E=1.2\times E_T^*$. As in previous x-ray scattering studies of the Q_1 CDW at higher temperatures,[24,27] the scan taken at ZF is clearly sharper than that taken at $1.2\times E_T^*$. In order to extract the characteristic length scales, we fit the data to the same line shape used by Ringland *et al.*,[24,27] which accurately describes both the pinned and sliding states of the Q_1 CDW at high temperatures. Specifically, we assume that

$$\lim_{t\to\infty} g(\boldsymbol{r},t)=\left(\frac{r}{\xi}\right)^{2\alpha}, \quad (3)$$

where ξ is the characteristic length scale describing the loss of phase coherence and α is the phase roughness scaling exponent. Larger values of α imply that the mean-square phase fluctuation grows more rapidly with distance, producing ''rougher'' CDW phase fronts. Figure 2(b) is a semilog plot of the same sliding state data shown in Fig. 2(a), but over a larger range of **q** to illustrate the high quality of the fit in the wings. Clearly, this functional form describes the data extremely accurately over a dynamic range of several decades. The pinned and sliding states of Q_2 have $\alpha\simeq0.5$, 0.8, respectively. These same line shapes describe the pinned and depinned states of Q_1 CDW between T_{p1} and T_{p2}.

We then systematically measured the structure of the Q_2 CDW as a function of applied field and temperature. Broadband noise (BBN) and dV/dI measurements were conducted *in situ* to determine E_T and E_T^*, respectively. The applied field was varied along a hysteresis loop which terminated at $\sim\pm2\times E_T^*$ to avoid significant Joule heating of the sample. Figure 3 shows the results obtained at 30 K. Each data point

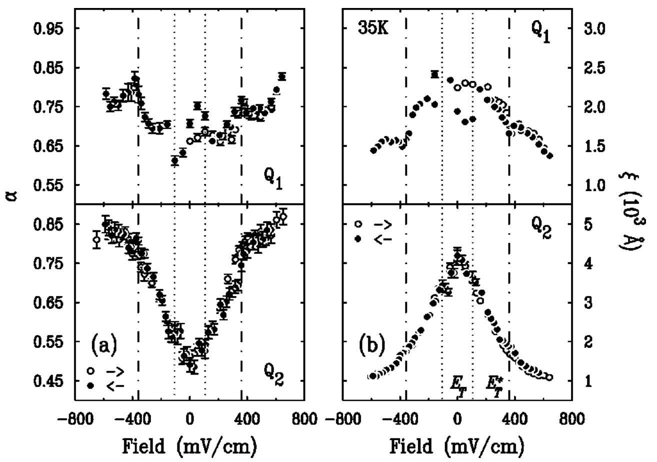

FIG. 4. Comparison of x-ray structure information for Q_1 (upper panels) and Q_2 (lower panels) CDW's at 35 K as a function of applied electric field. (a) Phase roughness exponent, α. (b) Correlation length, ξ. The two dashed lines indicate E_T and E_T^*.

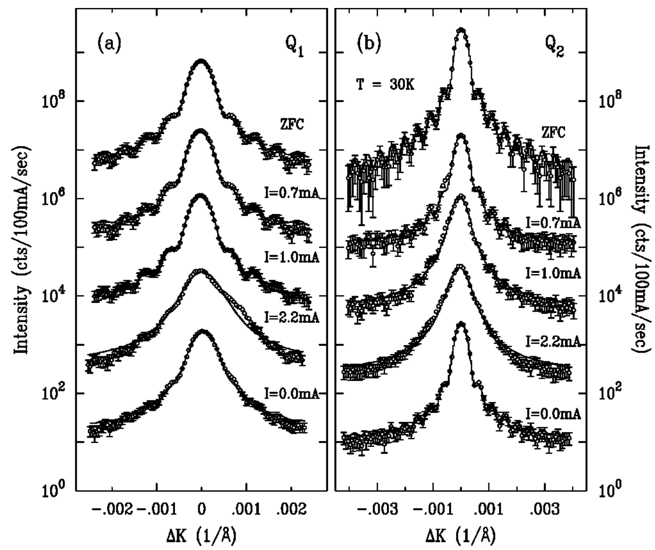

FIG. 5. Transverse scans of (a) Q_1 and (b) Q_2 CDW's at 30 K as a function of applied field. Applied total current $I=0.5$ mA and $I=1.5$ mA correspond to E_T and E_T^*, respectively. Solid lines are the best fit results to Eq. (3) convolved with the finite-size effect. Scans are offset for clarity.

indicates the best fit to an x-ray data set similar to that shown in Fig. 2.

For $E<E_T$, both ξ and α are constant within experimental errors. The best fit value, $\alpha\approx0.5$, implies an exponentially decaying phase-phase correlation function, consistent with the predictions of phase-only weak-pinning models based on the Fukuyama-Lee-Rice (FLR) Hamiltonian.[2,28,29] The correlation length $\xi\approx5000$ Å is the same order of magnitude but slightly larger than that measured on the Q_1 CDW at higher temperatures and is comparable to the sample thickness. For $E>E_T$, ξ decreases and α increases smoothly with increasing E. These results demonstrate that the structure of the Q_2 CDW is indistinguishable from that previously measured by Ringland *et al.*[24,27] on the Q_1 CDW in both the pinned and the sliding states. The absence of an abrupt change in the line shape of the Q_2 satellite at E_T^* is, however, somewhat surprising.

Searching for a structural signature of switching, we performed an additional series of measurements on both Q_1 and Q_2. Figure 4 shows the results obtained at 35 K. Contrary to the naive expectation, we observe a discontinuous change of the Q_1 CDW at E_T^* to the same line shape as the Q_1 CDW has in the sliding state above T_{p2}. Obtaining reproducible data sets was extremely difficult due to equilibration times much longer than the few days available for these experiments. However, the abrupt change at E_T^* is beautifully confirmed and explained by x-ray data collected at APS. In this series of measurements, rather than perform a cyclic series of electronic measurements, we began with the system carefully prepared in a zero-field cooled (ZFC) state. Due to the excellent coherence properties of the x-ray beam, finite-size (FS) oscillations[30] are present on both the Bragg peaks and the CDW satellites. As shown in Fig. 5, up to eight orders of oscillation are observed on the wings of the Q_2 satellite. The data are accurately described by simply fixing the limits of integration of Eq. (2) to reflect the size of the sample. The best fit of this line shape to the data is shown by the solid lines in Fig. 5 and the best fit values of the parameters agree extremely well with the measured sample thickness.

In the regime $E_T<E<E_T^*$, the center of the Q_2 satellite begins to broaden and the amplitude of the finite-size oscillations begins to drop. Meanwhile, the Q_1 satellite remains unchanged from its ZFC state. At $E\simeq E_T^*$, the Q_1 satellite abruptly broadens and becomes asymmetric. The FS oscillations on both CDW satellites are smeared out. Reducing the applied field back to zero causes the Q_2 satellite to sharpen and the FS oscillations are substantially, but not completely, recovered. The ZF state of the Q_2 CDW is more disordered than the ZFC state. In contrast, the Q_1 satellite remains very broad and does not recover any FS oscillations. These data thus provide an explanation for the difficulty in interpreting the Q_1 data collected in a cyclic fashion. The Q_1 CDW does abruptly change state as the applied electric field is increased through E_T^*; however, when the field is reduced through E_T^*, the kinetics of the structural relaxation are too slow to observe. This behavior is consistent with previous time-resolved x-ray-diffraction measurements on the Q_1 CDW at temperatures above T_{p2} which found a nearly exponential increase in the time constant for the relaxation of the Q_1 CDW from the sliding to the pinned state with decreasing temperature.[27] Extrapolating to these low temperatures, the relaxation time for Q_1 would be on the order of 10^4 s, two orders of magnitude longer than the time scales probed here.

These results are consistent with a Landau free-energy analysis[20,21] which reveals that the lowest-order symmetry-allowed term coupling the two CDW order parameters is fourth order in the CDW amplitudes; therefore, the effects of the coupling are predicted to be too small to observe in the *pinned* state. As suggested by Bruinsma *et al.*,[21] extending the theory to the dynamical case is likely to enhance the coupling, making it easier to observe.

This observed behavior of the Q_1 CDW raises the interesting question of what is going on at E_T^*. Based only on these x-ray data, one might be tempted to argue that the Q_1 CDW is coupled to the Q_2 CDW and that it is the depinning of the Q_1 CDW at E_T^* that is responsible for switching in $NbSe_3$. However, previous reports in the literature demonstrate that switching occurs in systems with only one CDW;[8–10] therefore, coupling is not appealing as a general explanation for switching. Furthermore, at temperatures above T_{p2}, E_T for Q_1 grows nearly exponentially with decreasing temperature. Extrapolating to T_{p2} suggests that the Q_1 CDW should not depin until applied fields significantly larger than E_T^*.[31]

Some insight into how Q_1 changes without sliding can be gained by considering what the Q_1 CDW ''feels'' in its rest frame. The Q_1 CDW could respond to *relative* motion between itself and the Q_2 CDW rather than to its motion relative to impurities or defects. The sliding of Q_1 could be detected by transport measurements since this implies a new set of charge carriers contribute to current flow. Lemay *et al.*[4] have already shown that nearly all of the Q_2 CDW condensate participates in the slow but coherent motion during current flow between $E_T < E < E_T^*$. The possibility of Q_1 sliding would be ruled out if no significant change is observed in the number of charge carriers as one crosses E_T^*. These challenging transport measurements are the subject of ongoing investigations.

In summary, we have shown that the Q_2 CDW depins at E_T, continuously entering a disordered state characterized by a smoothly increasing phase roughness exponent α and decreasing correlation length ξ. No dramatic structural change is observed at E_T^*. In contrast, the Q_1 CDW changes state abruptly at E_T^*, indicating a dynamic coupling between the Q_1 and Q_2 CDW's. This dynamic coupling and the slow kinetics of the Q_1 CDW may play an important role in the diverse phenomena observed in the switching regime.

This work was supported by NSF Grant Nos. DMR-98-01792 and DMR-97-05433. Use of the Advanced Photon Source was supported by the U.S. DOE under Contract No. W-31-109-Eng-38. We thank J. Jordan-Sweet and S. Lemara on beam line X20A at NSLS, and L. Lurio, J.F. Pelletier, and H. Gibson on 8-ID at APS for their technical help.

*On leave from Department of Materials Science and Engineering K-JIST, Korea.

[1] R. Peierls, *Quantum Theory of Solids* (Clarendon Press, Oxford, 1955).
[2] L. J. Sham and B. R. Patton, Phys. Rev. B **13**, 3151 (1976).
[3] See comprehensive reviews by P. Monceau, in *Electronic Properties of Quasi-One-Dimensional Materials* (Reidel, Dordrecht, 1985), Pt. II, p. 139; G. Gruner, Rev. Mod. Phys. **60**, 1129 (1988).
[4] S. G. Lemay, R. E. Thorne, Y. Li, and J. D. Brock, Phys. Rev. Lett. **83**, 2793 (1999).
[5] A. Zettl and G. Grüner, Phys. Rev. B **26**, 2298 (1982).
[6] J. Levy and M. S. Sherwin, Phys. Rev. B **43**, 8391 (1991).
[7] R. P. Hall, M. Sherwin, and A. Zettl, Phys. Rev. B **29**, 7076 (1984).
[8] R. M. Fleming *et al.*, Phys. Rev. B **33**, 5450 (1986).
[9] N. Maeda, A. M. Notomi, and K. Uchinokura, Phys. Rev. B **42**, 3290 (1990).
[10] M. E. Itkis, F. Y. Nad, and P. Monceau, J. Phys. C **2**, 8327 (1990).
[11] R. P. Hall, M. F. Hundley, and A. Zettl, Phys. Rev. B **38**, 13 002 (1988).
[12] T. L. Adelman *et al.*, Phys. Rev. B **47**, 4033 (1993).
[13] P. B. Littlewood, Solid State Commun. **65**, 1347 (1988).
[14] S. V. Zaitsev-Zotov, G. Remenyi, and P. Monceau, Phys. Rev. Lett. **78**, 1098 (1997).
[15] L. Balents and M. P. A. Fisher, Phys. Rev. B **75**, 4270 (1995).
[16] V. M. Vinokur and T. Nattermann, Phys. Rev. Lett. **79**, 3471 (1997).
[17] J. L. Hodeau *et al.*, J. Phys. C **11**, 4117 (1978).
[18] R. M. Fleming, D. E. Moncton, and D. B. McWhan, Phys. Rev. B **18**, 5560 (1978).
[19] P. A. Lee and T. M. Rice, Phys. Rev. B **19**, 3970 (1979).
[20] V. J. Emery and D. Mukamel, J. Phys. C **12**, L677 (1979).
[21] R. Bruinsma and S. E. Trullinger, Phys. Rev. B **22**, 4543 (1980).
[22] N. P. Ong, Phys. Rev. B **17**, 3243 (1978).
[23] R. M. Fleming, D. E. Moncton, J. D. Axe, and G. S. Brown, Phys. Rev. B **30**, 1877 (1984).
[24] K. L. Ringland *et al.*, Phys. Rev. B **61**, 4405 (2000).
[25] M. Sutton *et al.*, Nature (London) **352**, 608 (1991).
[26] R. E. Thorne, J. P. Tucker, and J. Bardeen, Phys. Rev. Lett. **58**, 828 (1987).
[27] K. L. Ringland *et al.*, Phys. Rev. Lett. **82**, 1923 (1999).
[28] H. Fukuyama and P. A. Lee, Phys. Rev. B **17**, 535 (1978).
[29] K. B. Efetov and A. I. Larkin, Zh. Éksp. Teor. Fiz. **72**, 2350 (1977) [Sov. Phys. JETP **45**, 1236 (1977)].
[30] B. E. Warren, *X-ray Diffraction* (Dover, New York, 1990).
[31] J. McCarten *et al.*, Phys. Rev. B **46**, 4456 (1992).